Title

Salicylic acid mitigates physiological and proteomic changes induced by the SPCP1 strain of Potato virus X in tomato plants

Permalink

https://escholarship.org/uc/item/2np869pt

Authors

Cueto-Ginzo, Ana Isabel
Serrano, Luis
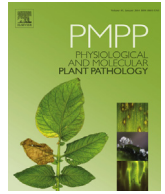Bostock, Richard M
et al.

Publication Date

2016

DOI

10.1016/j.pmpp.2015.11.003

Peer reviewed

Salicylic acid mitigates physiological and proteomic changes induced by the SPCP1 strain of *Potato virus X* in tomato plants

Ana Isabel Cueto-Ginzo [a, c], Luis Serrano [a, b], Richard M. Bostock [d], Juan Pedro Ferrio [a, b], Ricardo Rodríguez [a], Laura Arcal [a, c], María Ángeles Achon [a, b], Tania Falcioni [a], Walter Patricio Luzuriaga [c], Vicente Medina [a, b, *]

[a] Grupo INPLAMICVEC, Departament de Producció Vegetal i Ciència Forestal, Universitat de Lleida (UdL), Avda. Rovira Roure 191, 25198, Lleida, Spain
[b] AGROTECNIO Center, Universitat de Lleida, Avda. Rovira Roure 191, 25198, Lleida, Spain
[c] UdL-IMPULS Programme, Universitat de Lleida, Avda. Rovira Roure 191, 25198, Lleida, Spain
[d] Plant Pathology Department, University of California, Davis, CA, USA

ARTICLE INFO

ABSTRACT

Induction of resistance by salicylic acid (SA) exogenous treatment is a complementary approach to control plant diseases. SA effect on *Potato virus X* (SPCP1 strain) − infected tomato plants was examined by analyzing their physiological parameters and proteomic profiling at initial infection. PVX-SPCP1 altered photosynthesis and carbohydrate synthesis proteins and elicited stress proteins. SA partially offset reduction in photosynthetic rate during infection by increasing mesophyll conductance. SA counteracted these changes through stabilization of photosystem II, increased proteins related with thermotolerance and stress, and decreased proteins related with stomatal opening. The strongest effects of SA occurred at the beginning of the pathogenesis cycle.

© 2015 Elsevier Ltd. All rights reserved.

1. Introduction

Plant infection by microbial pathogens induces deep metabolic changes which may be identified by analyzing the plant transcriptome and corresponding proteome profiles. Studies about protein expression changes have led to the identification of complex biochemical pathways and mechanisms in several pathosystems such as the interaction between banana and *Fusarium oxysporum* f.sp. *cubense* [42]; sugar beet and either a traditional A-type strain or a Rz1 resistance breaking strain of *Beet necrotic yellow vein virus* (BNYVV) [36,67]; apple and the fungus *Colletotrichum gloeosporioides* [54], and many others.

Pathosystems in need of further investigation are those of *Potato virus X* (PVX), type member of the *Potexvirus* genus (Fam. *Alphaflexiviridae*), in different host plant species. PVX is one of the most common plant viruses and causes great economic losses to solanaceous crops around the world [1]. This virus induces mild to no symptoms, but increased symptom expression has been observed in mixed infections with other plant viruses [11,47].

Systemic acquired resistance (SAR) can provide long-term defense in plants against a broad-spectrum of pathogens. SAR is mediated by the phytohormone salicylic-acid (SA) [29], which is induced in plants in response to various abiotic and biotic stresses [30]. Exogenous application of SA affects many physiological processes such as transpiration rate [35], stomatal closure and regulation [45,52], membrane permeability [7], growth and photosynthesis [5,18,24], lignin deposition [22], and antioxidant capacity [3]. Although it has been established that endogenous SA interferes in three main stages of the plant virus cycle: cell-to-cell movement, long distance movement, and replication [2,46,58,61], the efficacy of exogenous SA treatment for plant virus diseases control needs to be adjusted for every plant viral pathosystem.

Although some effects of SA on PVX-infection in plants have been reported before [38], the relationships between physiological parameters and corresponding protein expression during plant virus infection is poorly known. Our previous work demonstrated a delay in viral infection for tomato plants inoculated with an asymptomatic PVX strain (CP4, accession no. AF172259.1) after a

---

* Corresponding author. Grupo INPLAMICVEC, Departament de Producció Vegetal i Ciència Forestal, Universitat de Lleida (UdL), Avda. Rovira Roure 191, 25198, Lleida, Spain.

E-mail address: medinap@pvcf.udl.cat (V. Medina).

previous application of SA [19]. Advancing our study and continuing to work in the context of considering SA as a disease control treatment, the work herein expands upon our findings by determining if continuous exposure of the plant to exogenous SA can retard or contain the infection by a PVX strain (SPCP1, accession no. KJ631111) that induces symptoms in tomato and is phylogenetically distanced from PVX-CP4. In the present research we evaluate plant growth and photosynthetic parameters in kinetic experiments, and compare leaf proteome profiles across different treatment combinations. Within this framework, we identify changes that occur in photosynthetic parameters of the leaf and in the tomato proteome when plants were treated with different concentrations of SA and infected by PVX (SPCP1 strain). This experimental design serves as part of a broader program in search of a deeper mechanistic understanding of the physiological and biochemical events that occur during the SA-plant-virus interactions.

2. Materials and methods

2.1. Plant material, growth conditions and PVX strain

Experiments were conducted in a growth chamber at constant temperature of 22 °C and 12 h photoperiod. Three tomato seeds (*Solanum lycopersicum* L. cv. Boludo) were sown in pots (500 cc) with autoclaved commercial substrate (Traysubstrat®, Klasmann-Deilmann, Gmbh, Geeste, Germany). After seedlings emerged, only one seedling was maintained per pot. For plant inoculation, a Spanish isolate of *Potato virus X* (PVX) (Accession number: KJ631111 corresponding to SPCP1strain) from lyophilized infected tomato tissue was used.

2.2. Experimental design, SA application and PVX inoculation

Experimental trials were carried out in six plots with 20 plants per plot, in a completely randomized design (TRD). Salicylic acid was applied by spraying the foliage of the plant with an aqueous solution at two dilutions, 1.5 mM (SA1) and 3.5 mM (SA2), of commercial salicylic acid (Rhodia, France). Treatment 1 was the negative control (no SA treatment nor PVX inoculation), treatments 2 and 3 corresponded to SA1 and SA2 respectively without PVX inoculation, treatments 4 and 5 were SA1 and SA2 respectively and PVX inoculation, and treatment 6 was PVX inoculation without SA treatment. The first SA treatment was applied when tomato plants were at the four true-leaf stage and thereafter SA was applied once a week during the experiment time period. Mechanical inoculation with PVX was performed two days after the first SA application in

both treated and non-treated plants. Sampling times and timelines for each analysis are detailed in Fig. 1.

2.3. PVX detection

Viral infection was detected by DAS-ELISA using a polyclonal antiserum against PVX (Loewe Biochemica GmbH) and a standard protocol [12]. The leaf adjacent to the inoculated leaf of 5 plants per treatment was collected and analyzed by the ELISA test at 5, 7, 12 and 14 dpi. Absorbance was measured at 405 nm using a Microplate Spectrophotometer (Biorad, model 680) and samples with absorbance levels that were at least three times the value of non-PVX inoculated tomato plants (negative control) were considered positive.

2.4. Plant growth and root analysis

The height of five tomato plants per treatment was measured at end of the experiment (16 days after the first SA application) and the roots of 3 plants per treatment were examined at 2dpt (days post SA treatment)/0dpi (days post inoculation with PVX), 7dpt/5dpi and 14dpt/12dpi. The roots were carefully washed with tap water to avoid tissue damage, and preserved in 50% ethanol (w/w) at 4 °C until further analysis. Root images were obtained with an Epson Perfection V700 modified flatbed scanner. Roots were analyzed for length, volume, surface area, number of tips, forks and average diameter using WinRHIZO software (version 2009; Regent Instruments Inc., Quebec, ON, Canada).

2.5. Analysis of physiological parameters

Photosynthetic rates (A) were obtained by an infrared gas analyzer (Walz GFS-3000, Heinz Walz GmbH, Effeltrich, Germany). The system was equipped with a LED-Array/PAM-Fluorometer 3055-FL and was set to follow growth-chamber conditions (photosynthetic active radiation: 500 μmol m^{-2} s^{-1}, relative humidity: 90% and C0$_2$ concentration: 500 ppm). Measurements were taken in 5 plants per treatment. Dark respiration (R_d) was estimated from measurements of net CO$_2$ exchange after switching off the light source for ca. 2min. Mesophyll conductance (g_m) was calculated from gas exchange values and fluorescence kinetics as described in Ref. [20]. Measurements were performed at 5, 7, 12 and 14 days post PVX-inoculation (dpi) (Fig. 1).

2.6. Total protein extraction

For proteomic analysis, one gram of leaf tissue per plant (3 plants per treatment) was collected and directly immersed in liquid nitrogen and stored at −80 °C. After this, 0.1 g of each sample was ground and 2 ml of 10% TCA (trichloroacetic acid (Sigma)) in acetone + 20 mM DTT (dithiothreitol; GEHealthcare) and protease inhibitor (complete ULTRA Tablets, Mini, EDTA-free, *EASYpack*, Sigma) was added and mixed by vortex. After centrifugation at 14,000 rpm at 4 °C for 30min, the supernatant was discarded and the pellet washed 3 times with 2 mL acetone +20 mM DTT and dried on ice (10−30 min). Total protein was eluted in 100−250 μL of lysis buffer (PER 4, Sigma). Protein content was measured by the Bradford method (Bio-Rad Protein Assay Dye Reagent Concentrate), using bovine serum albumin (BSA) as a standard.

2.7. Protein analysis

Total protein extracts containing 100 μg of total protein were separated by 2D-PAGE analytical gels. Three experimental replicates were performed for each treatment. For preparative gels,
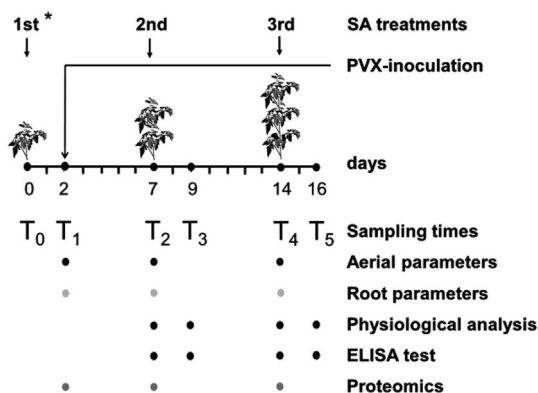

Fig. 1. Calendar of sampling and analysis (* at the tomato four true-leaf stage).

~500 μg of protein were applied. Samples were mixed with rehydration buffer (7 M urea, 2 M thiourea, 1% C7BzO detergent, 40 mM Trizma Base, 50 mM DTT, 1% IPG buffer pH 3—10 (GEHealthcare), and 0.002% bromophenol blue) in a total volume of 200 μL.

After testing several conditions, the following protocol for 2-DE gels was used: Isoelectric focusing (IEF) of passively rehydrated 18-cm IPG strips (pH 5—8) was performed in a Protean IEF Cell system (Bio-Rad) following the manufacturer's instructions. IEF used a sequential gradient procedure of 50 V/20° C/14 h. The current limit was 50 μA per IPG strip. Focused strips were stored at −80° C until the second dimension was performed. After IEF separation, the gel strips were incubated for 15min in the equilibration buffer (375 mM Tris base, 6 M urea, 20% glycerol, 2% SDS) containing 2% DTT, followed by 15min in the same buffer containing 2.5% iodoacetamide instead of DTT. Two equilibrated 18-cm gel strips were loaded in each 12.5% polyacrylamide gel (22 cm × 20 cm × 1 mm) for the second-dimension separation in an Ettan DALTsix Electrophoresis Unit (GE Healthcare). Electrophoresis was carried out in SDS-PAGE gels of 12.5%. Gels were stained with Flamingo™ Gel fluorochrome (Bio-Rad) according to the manufacturer's instructions. Image was acquired with the Versadoc MP4000 system (Bio-Rad).

2.8. In-gel protein digestion and MS analysis

Selected spots were manually excised from gels, digested with trypsin using 96-well perforated plates and a MultiScreen™ HTS Vacuum Manifold (Millipore). Each gel piece containing the protein was minced, washed twice with deionized water and dehydrated with 50% ethanol in 50 mM NH_4HCO_3 for 10min, and then with 100% ethanol for 10 min.

Gel pieces were then reduced with 10 mM DTT in 50 mM NH_4HCO_3 for 1 h at 56 °C and alkylated with 55 mM iodoacetamide in 50 mM NH_4HCO_3 for 30 min at room temperature in the dark. After this, the gel pieces were washed twice in 50 mM NH_4HCO_3 for 15min and dehydrated with 5% acetonitrile (ACN) in 25 mM NH_4HCO_3 for 15min, 50% ACN in 25 mM NH_4HCO_3 for 15min twice and finally with 100% ACN for 10min. After total CAN evaporation, 15 μl of 20 ng μl^{-1} trypsin in 25 mM NH_4HCO_3 was added and left at 4 °C for 45min to allow full rehydration of gel pieces with the trypsin solution. The gel pieces were then covered with 25 mM NH_4HCO_3 and incubated at 37 °C overnight for proteolysis. Following digestion, eluted peptides were transferred to a new Eppendorf tube. One μl of the digested protein was used for a first peptide mass fingerprints (PMFs) analysis. If necessary, the minced gel was washed three times more with 0.25% trifluoroacetic acid (TFA) in 50% v/v ACN, twice with 100% ACN, evaporated in a SpeedVac (Savant) and then re-suspended in 5 μl of 70% ACN- 0.1% TFA to collect remaining peptides. One microliter μl of peptide solution was spotted per well on a MALDI target, and allowed to evaporate at room temperature before being covered with 1 μl of a saturated solution of α-cyano-4-hydroxycinnamic acid prepared in 50% v/v ACN containing 1% TFA. Mass calibrations were carried out using a standard peptide mixture. Mass spectra were acquired using Autoflex Speed MALDI-TOF/TOF mass spectrometer (Bruker Daltonics). The experimental design had three biological repetitions with three experiments each.

2.9. Database search and protein identification

Protein identification was performed using MALDI-TOF mass fingerprint (PMF) and MALDI-TOF/TOF. PMF and MS/MS spectra were compared against SwissProt, Plants EST, and NCBInr and TrEMBL databases, using the search engine MASCOT algorithm (Version 2.4, Matrix Science, London, UK). The following

parameters were used for PMF database searches: monoisotopic peptide masses; allowed modifications, cysteine carbamidomethyl (fixed), oxidation of methionine (variable); one trypsin missed cleavage and a maximum of ±100 ppm mass accuracy. Search parameters used for MS/MS searches were also the same as for PMF with a maximum MS/MS tolerance peptide of ±0.4 Da.

2.10. Statistical analysis

Statistical analyses of physiological data were performed using the JMP® software version 8.0 (SAS Institute, Cary, NC USA). The analysis was carried out separately for each sampling time (see Fig. 1). The interaction between PVX-SPCP1 and the different SA doses was evaluated for each parameter measured. To separate means a Fisher's Least Significant Difference (LSD) was conducted.

Spot detection and gel analysis was first conducted with the PDQUEST program (Bio-Rad) and the second time, manually. Normalization was performed with the regression model LOESS [15]. Only the spots present on all of the gel replicates were used for statistical analysis. Ratios between two expressed conditions were calculated as the mean of three independent values for each spot from the 2D gel electrophoresis analysis ± standard error. Spots lacking quantitative signal or too high quantitative variation between replicates, or spots with mixed proteins, were not considered for further analysis.

3. Results and discussion

3.1. PVX detection

DAS-ELISA confirmed that PVX-inoculated plants were infected and SA treatment (overall) caused a delay for immuno-detection of PVX-SPCP1 up to 14dpt (Fig. 2), consistent with our previous study with the asymptomatic strain, PVX-CP4 [19]. Most likely, SA treatment delayed the systemic movement of the virus (since only systemic leaves were analyzed with the time-course experiment). Infected tomato plants without SA treatment showed the mosaic symptoms typically induced by PVX-SPCP1. However, the SA-induced delay in virus detection was earlier for PVX-SPCP1 than in previous work for PVX-CP4. The induction of symptoms and more rapid virus detection by ELISA, is probably on account of more rapid systemic movement, indicating that the SPCP1-PVX strain is more virulent and aggressive than the asymptomatic CP4-PVX strain; findings consistent with the suggested relationship
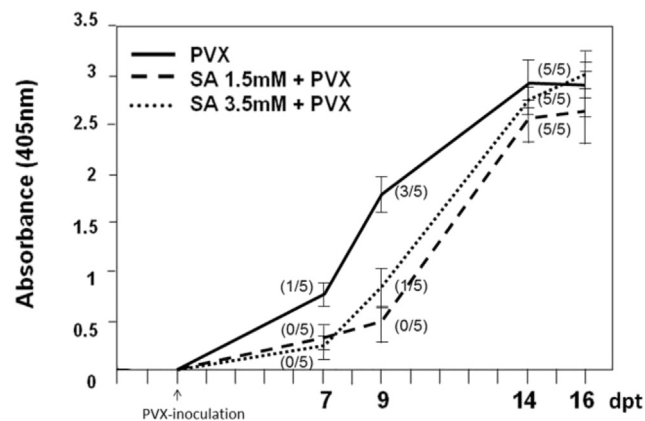

Fig. 2. Absorbance values in DAS-ELISA of *Potato virus X* (SPCP1 strain)-infected (cv. Boludo) plants untreated and treated with different doses of salicylic acid (SA). Number of positive plants/number of total analyzed plants is indicated in brackets. Absorbance values represent the average of 5 plants per trial.

between symptom severity and coat protein phylogenetic distance among these PVX strains [16].

3.2. Effects of SA and PVX infection on plant growth

Plant height values measured at the end of the experiment were significantly different ($p < 0.1$) between treatments. PVX-SPCP1 did not seem to have an effect on plant height relative to the control but SA (1.5 mM) increased plant height; even a slight difference was observed in plants that were treated with the higher level of SA (3.5 mM) (Fig. 3). Significant differences ($p < 0.05$) were found in root length and root volume between control plants and SA-treated plants at 7 days post-treatment (dpt)/5 days post PVX inoculation (dpi) with the 3.5 mM SA dose (Fig. 4 and S1). However, there were no significant differences ($p < 0.05$) for this parameter at the end of experiment. Other parameters such as number of root tips or root bifurcations showed similar variation among treatments (data not shown). The initial negative effect on growth of exogenous salicylic acid treatment has been well established, as such that SA action on growth depends on developmental stage and the SA concentrations tested [53]. In our experiment, both doses (1.5 mM and 3.5 mM) slightly stunted plant growth (height of plant, length and volume of roots) during the initial stages of development. However, by the end of the experiment, SA-treated plants had recovered with the lower dose (1.5 mM) resulting in a small increase in plant height (Figs. 3 and 4 and S1). Thus, the initial negative effect of exogenous SA pre-treatment (especially in the higher dose, 3.5 mM) and later recovery observed in tomato plants are reasonable within the broader context of the reported effects of SA in plants.

3.3. Physiological parameters

PVX-infected plants had lower photosynthetic rate (A) values, which were maintained in all SA-treated plants. Combining values at 7, 12 and 14 dpi, ANOVA indicated a significant negative effect of PVX infection on photosynthesis ($p = 0.0017$) and a weak
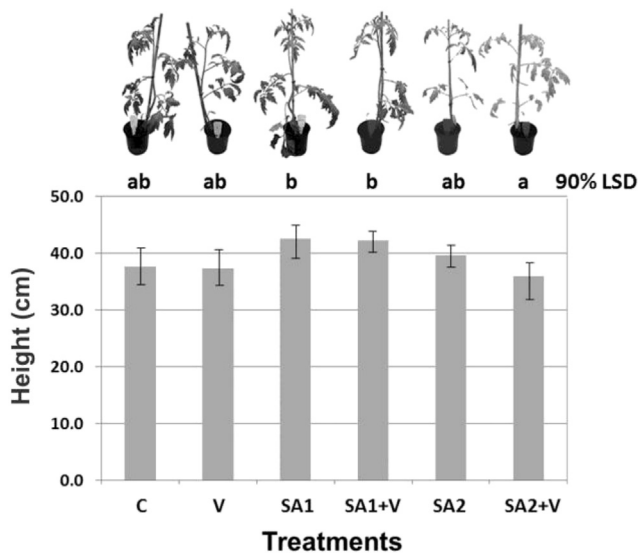
Fig. 3. Height of tomato (cv. Boludo) plants (average of 5 per trial) at the end of experiment (16 days post-SA treatment, 14 days post-PVX-SPCP1 strain inoculation). Means with different letters are significantly different (p < 0.1) (C: Control. Non-inoculated plants and no SA (salicylic acid) treatment applied. V: PVX (*Potato virus X*) -inoculated plants. SA1. Non-inoculated plants treated with SA 1.5 mM SA1 + V: PVX-inoculated plants treated with SA 1.5 mM SA2. Non-inoculated plants treated with SA 3.5 mM SA2 + V: PVX-inoculated plants treated with SA 3.5 mM).

Fig. 4. Root length of tomato plants (cv. Boludo) (average of 3 per trial) treated with different doses of salicylic acid (SA) at sampling times T_1 (7 dpt/5 dpi) and T_4 (14 dpt/12 dpi). Means with different letters are significantly different (p < 0.05) (C: Control. Non-inoculated plants and no SA (salicylic acid) treatment applied. V: PVX (*Potato virus X*) -inoculated plants. SA1. Non-inoculated plants treated with SA 1.5 mM SA1 + V: PVX-inoculated plants treated with SA 1.5 mM SA2. Non-inoculated plants treated with SA 3.5 mM SA2 + V: PVX-inoculated plants treated with SA 3.5 mM).
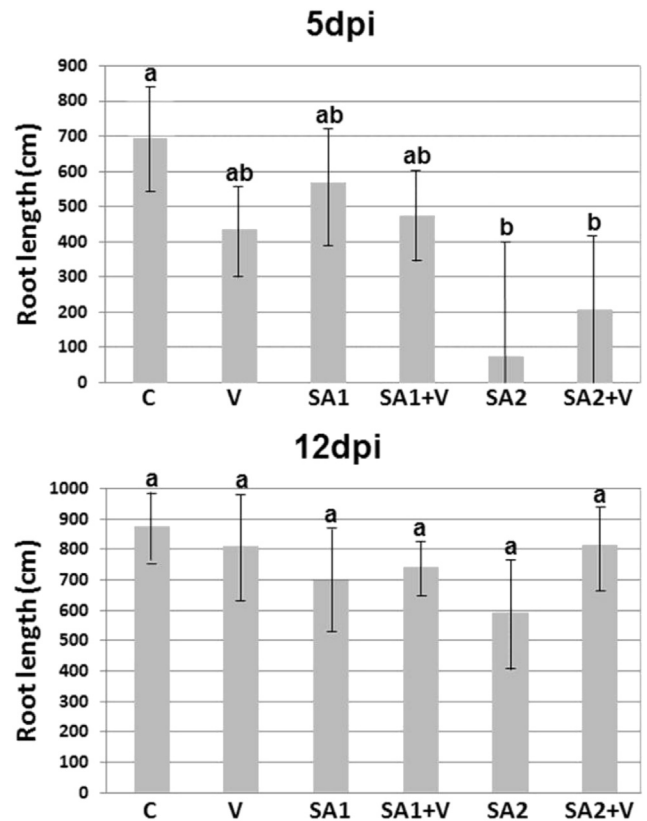
interaction in which the photosynthetic rate increased in PVX-infected plants after SA treatment ($p = 0.0842$; Fig. 5A). Similarly, the mesophyll conductance (g_m) increased significantly in PVX-infected plants after SA treatment ($p = 0.0081$; Fig. 5B). In contrast, dark respiration (R_d) increased in uninfected plants treated with SA and was unchanged in PVX-infected plants regardless of SA treatment (Fig. 5C). As in previous work with the CP4-PVX strain [19], SA restores the photosynthetic rate in SPCP1-PVX-infected tomato plants. According to results in the present study, this recovery could be attributed to a rise in mesophyll conductance (g_m), as previously reported in other plant-virus pathosystems [8,21,56]. Conversely, although SA treatment induced an increase in R_d, potentially associated to the stimulation of alternative oxidase pathways [40], this was only observed in the control plants, and does not explain the reported changes in photosynthetic rates. Furthermore, stomatal conductance (g_s) did not show significant differences between healthy and PVX-infected plants for any SA dose tested (data not shown).

3.4. Protein expression changes

Separation by 2-D gel electrophoresis of leaf protein extracts and comparative analysis with PDQuest software detected 85 non-redundant, differential spots from the various treatments. Sixty-one of these (78%) were identified by tandem mass spectrometry (Table 1). Fig. 6 shows spot location of the differentially expressed proteins in the tomato leaf proteome. Tables 2 and 3 show up or
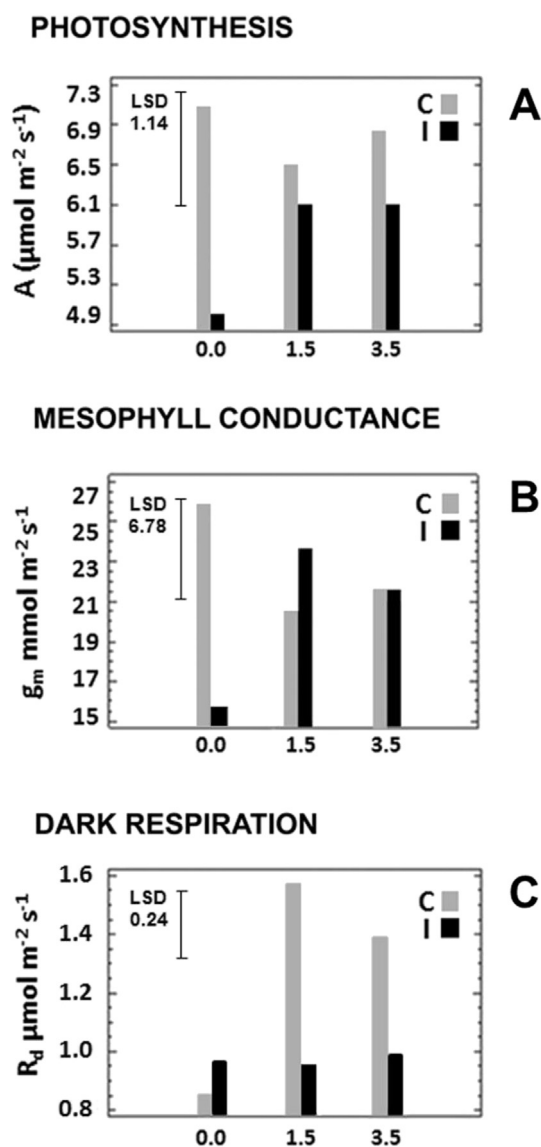
PHOTOSYNTHESIS

MESOPHYLL CONDUCTANCE

DARK RESPIRATION

Fig. 5. Interaction plots of tomato (cv. Boludo) plants *Potato virus X* (PVX)—infected (I), or non-infected (C, healthy), treated with different doses of salicylic acid (SA). A. Photosynthesis (A values). B. Mesophyll conductance (g_m values). C. Dark respiration (R_d values). Mean differences larger than the LSD value are significant at $p < 0.05$ (represented values are the result of combining three sampling times T_3, T_4 and T_5, meaning 7, 12 and 14 dpi, respectively).

down regulation of protein expression observed in the experiment in which SA at 1.5 mM produced consistent results. Comparison of the proteomes of healthy, SA-treated (1.5 mM), and PVX-infected tomato plants at different sampling times showed that most differentially expressed proteins are involved in photosynthesis, electron transport, and plant stress responses, rather consistent with physiological changes induced by SA in our experiments and reported in other plant-virus interactions [8,45]. Only values and comparisons with significant differences are shown in Tables 2 and 3, and almost null values are excluded. All values, including protein variation in controls, are shown in the supplementary table for reference.

3.5. Primary metabolism

Proteins involved in ATP synthesis, glycolysis, carbohydrate

biosynthesis and primary metabolism regulator were induced in all treatments: SA treated, SA + V, and virus inoculated plants, suggesting activation of metabolic pathways related with energy availability and molecule biosynthesis (Tables 2 and 3). Plant responses from secondary metabolism have been intensively studied for decades, but less is known about the effect of phytopathogens on plant primary metabolism [69]. Recently, interest in this aspect of plant viral interactions has been increasing as, for instance, in the potyviruses [59,68].

3.6. Photosynthesis

One effect of pathogen invasion is altered photosynthetic and carbohydrate metabolic patterns, like ferredoxin-NADP-reductase (FNR), reflected as an incremental demand for assimilation by the plant tissues, is evidenced in the present study (Table 3).

Another effect is that a large number of spots showing variation were related with RuBisCo proteins. We detected the RuBisCo enzyme complex involved in photosynthesis. It showed variations in the different treatments but it is difficult to compare them because the variation was too high between biological replicates. Overall, PVX-SPCP1-infection reduced the levels of RuBisCo fragments except in the case of RuBisCo small chain 3A/3C, where the effect was the opposite.

Another two proteins related with photosynthesis were downregulated in PVX-SPCP1-infected plants: photosystem II oxygen-evolving complex protein 3 and photosystem I reaction center subunit II. Down regulation of effective photosystem II quantum yield has been reported for viruses such as *Tobacco mosaic virus* and *Abutilon mosaic virus* [41], which is further confirmed by the physiological parameters measured in the present study. The inhibition of e—photosynthetic transport observed in virus infected plants is considered to be a result of reduction in the levels of proteins contributing to PSII [39], and mainly those related to the lysis/water oxidation complex [50]. Hence, it is novel that we observed a tendency for recovery in the photosystem II oxygen-evolving complex protein 3 in PVX-SPCP1-SA-treated plants (Table S1) that finally exhibited similar photosynthetic levels to healthy ones. SA treatment overall therefore seems to palliate, but not significantly recover reduced photosynthesis in infected plants.

The observed variation in protein levels related to Photosystem II (PSII) following SA treatment, including chlorophyll a-b binding protein 8, indicates that SA could play a role in the photosynthetic electron transport pathway, as reported by Ref. [31]. But, this effect was only clear after the first SA treatment, and there was no more significance during the course of observation (Table 2).

A homolog to plastidic aldolases increased in abundance after two SA (pre- and post-virus inoculation) treatments (Table 2). According to Ref. [26] a moderate decrease in plastid aldolase activity inhibits photosynthesis in potato plants. Thereby plastid aldolase increment following continuous exogenous SA treatment seems to improve photosynthesis. Although un-significant, PVX-SPCP1-infected plants showed a tendency to have lower aldolase levels compared with plants pre-treated with SA (Table 3). These findings may be indirectly related to physiological data of photosynthetic recovery of virus-infected plants because of SA treatment.

Levels of another protein, chloroplast sedoheptulose-1.7-bisphosphatase (SBPase), which is a ferredoxin/thioredoxin regulator involved in the chloroplast photosynthesis pathway [44,55], significantly increased following SA post-treatment of PVX-infected plants in one instance. Alternatively, in healthy plants, SBPase levels decreased overall, though they did significant increase after one SA pre-treatment. The chloroplast photosynthesis pathway requires light to reduce NADP, which in turn reduces ferrodoxin/thioredoxin, and subsequently SBPase. SBPase is converted it into

Table 1
Main characteristics and referred function of identified proteins in the PVX-SPCP1/tomato pathosystem, showing variation between treatments and corresponding to marked spots in Fig. 6.

SSP[a]	Protein	Accession no.[b] (Database)	Molecular weight (Da)/pI[c]	Coverage %	No peptides matched/Total peptides	Score[d]	Function
3104	Superoxide dismutase [Cu−Zn] 1	P14830*	15408/5.83	44	6/11	89	Antioxidant defense
	Superoxide dismutase [Cu−Zn] 2	Q43779*	15346/5.65	44	6/11	89	
5202	Superoxide dismutase [Mn],	P35017*	25880/7.10	3 ·	1	21	Antioxidant defense
4604	Monodehydroascorbate reductase	Q43497*	47120/5.77	5 ·	3	76	Antioxidant process
2801	ATP synthase subunit alpha	Q2MIB5*	55434/5.14	26	15/34	208	ATP synthesis
2812	ATP synthase subunit alpha	Q2MIB5*	55434/5.14	27	14/31	145	ATP synthesis
2702	ATP synthase subunit beta	Q2MI93*	53491/5.28	60	27/72	195	ATP synthesis
	Ribulose bisphosphate carboxylase large chain	P27065*	53434/6.55		18/72		
3103	ATP synthase epsilon chain	Q2MI94*	14571/5.43	54	7/24	105	ATP synthesis
6006	ATPase-like	ABB86274**	12502/6.75	64	7/8	136	ATP synthesis
4204	Chlorophyll a-b binding protein 8	P27522*	29344/8.96	21 ·	4	282	Energy distribution
6206	Ethylene receptor 1	Q41342*	84715/7.99	24	19/30	162	Ethylene signaling regulator
1603	chloroplast sedoheptulose-1,7-bisphosphatase	NP_001234585**	43017/6.07	46	18/67	181	Ferredoxin/Thioredoxin regulator
1605	chloroplast sedoheptulose-1,7-bisphosphatase	ACR46521**	43017/6.07	37	18/38	174	Ferredoxin/Thioredoxin regulator
1610	chloroplast sedoheptulose-1,7-bisphosphatase	NP_001234585**	43017/6.07	46	19/26	233	Ferredoxin/Thioredoxin regulator
7505	glyceraldehyde 3-phosphate dehydrogenase	NP_001234803**	32297/6.33	33	10/26	87	Glycolysis Apoptosis Golgi vesicle shuttling
5103	Solanum lycopersicum cDNA, clone	BP903052***	17598/6.99	25 ·	3	199	Interconversion of peptides in proline
	Peptidyl-prolyl cis-trans isomerase	B9RMA****	27656/9.58	15 ·	3	193	
7101	Peptidyl-prolyl cis-trans isomerase	C5YXY3****	26347/9.26	7 ·	1	127	Interconversion of peptides in proline
5207	Glutathione S-transferase, class-phi	AAB65163**	23809/5.81	4 ·	1	54	Multifunctional intercellular
7407	Proteasome subunit alpha type-7	O24030*	28577/8.41	42	14/34	138	Pathogen interaction
3504	Ferredoxin–NADP reductase, leaf-type isozyme	O04977*	40705/8.37	41	16/38	151	Photosynthesis e− transport
4404	Putative ferredoxin-NADP reductase	AAX57356**	35442/7.71	54	16/48	122	Photosynthesis e− transport
5403	Putative ferredoxin-NADP reductase (Fragment)	Q4KQT2****	35469/7.71	60	18/24	232	Photosynthesis e− transport
4507	NAD(P)H-quinone oxidoreductase subunit H	Q2MI44*	45746/5.30	20	9/23	78	Photosynthesis e− transport
1201	Oxygen-evolving enhancer protein 2	P29795*	27946/8.26	47	11/25	149	Photosynthesis
1208	Oxygen-evolving enhancer protein 2	P29795*	27946/8.26	34	8/40	87	Photosynthesis
2203	Oxygen-evolving enhancer protein 2	P29795*	27946/8.26	17 ·	3	110	Photosynthesis
5404	Oxygen-evolving enhancer protein 1	P23322*	35154/5.91	23	6/19	72	Photosynthesis
3505	Homologous to plastidic aldolases	CAA71408**	38632/5.89	6 ·	2	121	Photosynthesis regulation
9112	Photosystem II oxygen-evolving complex protein 3	NP_001234528**	24557/9.64	55	16/62	166	Photosynthesis Primary energy
9114	Photosystem I reaction center subunit II	P12372*	22961/9.71	32	9/61	109	Photosynthesis Primary energy
3808	Ribulose bisphosphate carboxylase large chain	P27065*	53434/6.55	22	11/56	79	Photosynthesis Respiration
	Transketolase	Q43848*	80341/5.94	17	12/56	72	Carbohydrate biosynthesis
	Stromal 70 kDa heat shock-related protein	Q02028*	75583/5.22	19	11/56	58	Protein folding, Protein transport
1609	Ribulose bisphosphate carbox./oxygenase activase	O49074*	50897/8.61	50	29/44	314	Photosynthesis Respiration
2607	Ribulose bisphosphate carbox./oxygenase activase	O49074*	50897/8.61	38	18/48	170	Photosynthesis Respiration
3605	Ribulose bisphosphate carbox./oxygenase activase	O49074*	50897/8.61	43	21/48	228	Photosynthesis Respiration
3612	Ribulose bisphosphate carbox./oxygenase activase	O49074*	50897/8.61	34	18/44	187	Photosynthesis Respiration
4502	Ribulose bisphosphate carbox./oxygenase activase	O49074*	50897/8.61	50	26/56	245	Photosynthesis Respiration
4603	Ribulose bisphosphate carbox./oxygenase activase	O49074*	50897/8.61	47	24/34	304	Photosynthesis Respiration
5603	Ribulose bisphosphate carbox./oxygenase activase	O49074*	50897/8.61	31	14/38	144	Photosynthesis Respiration
6608	Ribulose bisphosphate carbox./oxygenase activase	O49074*	50897/8.61	41	27/37	324	Photosynthesis Respiration
4101	Ribulose bisphosphate carbox. small chain 3A/3C	P07180*	20446/6.73	46	9/36	108	Photosynthesis Respiration
4811	Ribulose bisphosphate carboxylase large chain	P27065*	53434/6.55	24	12/38	115	Photosynthesis Respiration
6808	Ribulose bisphosphate carboxylase large chain	P27065*	53434/6.55	6 ·	3	54	Photosynthesis Respiration
6809	Ribulose bisphosphate carboxylase large chain	P27065*	53434/6.55	1	1	42	Photosynthesis Respiration
7809	Ribulose bisphosphate carbox./oxygenase large sub.	YP_514860**	53434/6.55	38	18/55	162	Photosynthesis Respiration

Table 1 (*continued*)

SSP[a]	Protein	Accession no.[b] (Database)	Molecular weight (Da)/pI[c]	Coverage %	No peptides matched/Total peptides	Score[d]	Function
1509	BP903634.1 Solanum lycopersicum cDNA, clone	BP903634***	17176/9.39	83	16/23	252	Photosystem II stability
	Plastid high chlorophyll fluorescence 136 precursor	ABQ53629**	43064/8.71	5	2(1)	73	Assembly factor HCF136
5104	Wound-inducible carboxypeptidase precursor.	NP_001234691**	56039/5.84	1 •	1	63	Plant defense
	Putative uncharacterized protein *Vitis vinifera*	A5AIJ0****	54166/5.63	6 •	3	87	Unknown
9003	Pathogenesis-related leaf protein 6	P04284*	17965/8.86	43	7/21	99	Plant defense
4408	AW040417.1 EST283281 tomato mixed elicitor	AW040417***	24746/9.80	5 •	1	86	Plant defense elicitor
5001	Probable phospholipid hydroperoxide glutathione peroxidase	O24031*	19007/6.58	25	5/16	67	Peroxidase PR9-like
5308	Triose phosphate isomerase (cytosolic isoform)	AAR11379**	27251/5.73	11 •	2	155	Primary metabolism regulator
5509	mRNA binding protein precursor	gi|350534514**	44084/7.10	30	10/57	75	Product as response to wounding
4512	mRNA binding protein precursor	NP_001234656**	44084/7.10	38	21/45	228	Product as response to wounding
4301	Chaperonin 21 precursor	NP_001234423**	26603/6.85	3 •	1	61	Protein folding ATP binding
4803	Heat shock protein 70	NP_001233780**	74415/5.41	21	14/55	75	Protein folding
3904	Luminal-binding protein	P49118*	73475/5.10	34	26/52	209	Protein folding
7503	Isovaleryl-CoA dehydrogenase 1	Q9FS88*	45640/7.94	36	15/35	155	Aminoacid degradation
6802	Subtilisin-like protease precursor	NP_001233982**	79565/6.25	26	16/22	193	Proteolysis
6804	Subtilisin-like protease precursor	NP_001233982**	79565/6.25	32	21/43	192	Proteolysis
4205	Temperature-induced lipocalin	NP_001234832**	21303/5.96	18 •	3	110	Thermotolerance component
5201	BG125080.1 EST470726 tomato shoot/meristem	BG125080***	25967/9.18	6 •	3	297	Protein coding Auxin-binding protein
6002	FS002771.1 Solanum melongena mRNA, clone	FS002772***	18090/8.58	9 •	1	116	Protein coding Ribosomal protein
8101	BP903052.1 Solanum lycopersicum cDNA, clone	BP903052***	17598/6.99	56	10/40	134	Unknown Protein Coding folding

[a] Spot numbers refer to Fig. 6 identified either by fingerprint mass spectrometry MS (MALDI-TOF) or by MS/MS (MALDI TOF-TOF) (•).
[b] Accession number and molecular mass according to SwissProt database (us.expasy.org/sprot)*, NCBI**, Plant EST*** and TrEMBL****.
[c] MW and pI were calculated from amino acid sequence.
[d] Scores of proteins identified by peptide mass fingerprinting were determined according to Mowse values obtained either from MASCOT.
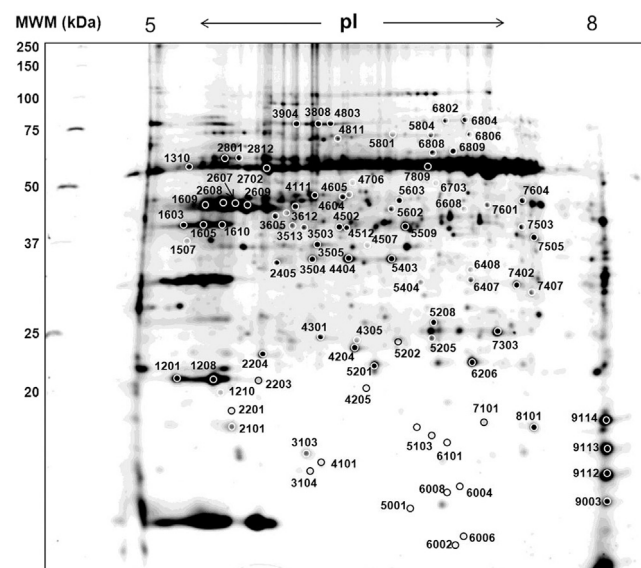

Fig. 6. Representative 2-D PAGE gel image of tomato leaf (cv. Boludo). Total soluble leaf proteins were electro-focused on an IPG strip (pH-4–8) and resolved on 12% (w/v) SDS-PAGE. Molecular markers are indicated as kDa. The representative spots of Table 1, those showing variation between treatments, are indicated in the gel circles and their numbers.

its active form, found to have a strong correlation with increased photosynthetic carbon fixation activity [48]. The inverse effect of SBPase in healthy vs. SA and SA-PVX infected plants thus vindicates the positive effect of SA treatment on the photosynthetic process. Perhaps this finding could be a better base for exploring a concrete relationship between SA, virus infection and photosynthesis.

In summary, SA has an indirect positive influence on photosynthesis by increasing expression of proteins involved in photosynthetic electron transport as well as the levels of plastid aldolase, RubisCo complex and SBPase (see Table 2 and Supplementary Table S1).

3.7. Plant stress responses

Expression levels of some biotic and abiotic stress-related proteins significantly changed during the course of the experiments. The ethylene receptor 1 (ETR1), a receptor transferase implicated in cell wall callose deposition during defense [49,51], was increased four-fold in tomato plants after two SA treatments (pre- and post-) and six-fold upon PVX-SPCP1 infection. PVX-infected plants + SA post-treatment then down-regulated and exhibited less relative ETR1; with levels similar to those of healthy plants. ETR1 expression levels may therefore indicate that cell wall callose deposition is an important response induced by SA and PVX-SPCP1 infection in tomato plants. This finding is in concordance with previous work, which pins ETR1 as a redundant negative regulator responsible for inhibiting ethylene production and causing a decrease in

Table 2
Variation of altered protein levels between healthy (C) and SA (salicylic acid dose: 1.5 mM) treated tomato (cv. Boludo) plants and SA treatment in time. Sub-index numbers indicate sampling times: $T_1 = 2$ dpt/0 dpi, $T_2 = 7$ dpt/5 dpi and $T_4 = 14$ dpt/12 dpi. Only values where differences were consistent (variation coefficient $\leq 50\%$ among replicates, spots present in all measured conditions, expression ratios ≤ 0.5 or ≥ 2.0, and *in visu* validated spots) are shown (T_1 corresponds with one SA treatment and T_2 and T_4 with two SA treatments, see Fig. 1).

SSP[a]	Protein	Ratio (SA/C)T_1	Ratio (SA/C)T_2	Ratio (SA/C)T_4	Ratio SAT$_4$/SAT$_2$
3104	Superoxide dismutase [Cu−Zn] 1 and [Cu−Zn] 2	17.06 ± 2.81	N.S.	N.S.	N.S.
5202	Superoxide dismutase [Mn]	5.95 ± 2.02	N.S.	0.13 ± 0.01	N.S.
2801	ATP synthase subunit alpha	N.S.	N.S.	3.14 ± 0.38	N.S.
2702	ATP synthase subunit beta	0.10 ± 0.01	N.S.	7.81 ± 2.19	N.S.
3103	ATP synthase epsilon chain	N.S.	N.S.	N.S.	N.S.
4204	Chlorophyll a-b binding protein 8	4.47 ± 1.46	N.S.	N.S.	N.S.
6206	Ethylene receptor 1	N.S.	N.S.	4.08 ± 0.22	N.S.
1603	Chloroplast sedoheptulose-1.7-bisphosphatase	0.50 ± 0.12	N.S.	N.S.	N.S.
1605	Chloroplast sedoheptulose-1.7-bisphosphatase	0.37 ± 0.05	N.S.	2.28 ± 0.10	3.92 ± 0.43
1610	Chloroplast sedoheptulose-1.7-bisphosphatase	0.10 ± 0.02	21.76 ± 14.6	8.12 ± 1.47	N.S.
5207	Glutathione S-transferase. class-phi	–	N.S.	0.37 ± 0.03	N.S.
3504	Ferredoxin–NADP reductase	N.S.	N.S.	N.S.	26.3 ± 18.1
4404	Putative ferredoxin-NADP reductase	N.S.	N.S.	N.S.	3.28 ± 1.78
5403	Putative ferredoxin-NADP reductase (Fragment)	N.S.	N.S.	N.S.	2.08 ± 0.95
4507	NAD(P)H-quinone oxidoreductase subunit H	N.S.	N.S.	N.S.	1.55 ± 0.29
1201	Oxygen-evolving enhancer protein 2	N.S.	N.S.	5.35 ± 0.57	N.S.
1208	Oxygen-evolving enhancer protein 2	0.48 ± 0.07	3.96 ± 1.87	4.69 ± 2.07	N.S.
5404	Oxygen-evolving enhancer protein 1	N.S.	N.S.	0.43 ± 0.16	N.S.
3505	Homologous to plastidic aldolases	0.27 ± 006	N.S.	2.49 ± 0.52	N.S.
9112	Photosystem II oxygen-evolving complex protein 3	N.S.	N.S.	0.17 ± 0.01	N.S.
2607	Ribulose bisphosphate carbox./oxygenase activase	N.S.	N.S.	0.48 ± 0.03	N.S.
3605	Ribulose bisphosphate carbox./oxygenase activase	0.01 ± 0.001	–	2.80 ± 1.05	–
6808	Ribulose bisphosphate carboxylase large chain	0.02 ± 0.01	–	–	–
6809	Ribulose bisphosphate carboxylase large chain	0.31 ± 0.04	N.S.	1.54 ± 0.82	N.S.
7809	Ribulose bisphosphate carbox./oxygenase large sub.	0.11 ± 0.01	N.S.	4.11 ± 1.20	N.S.
5104	Wound-inducible carboxypeptidase precursor	1.67 ± 0.90	N.S.	0.18 ± 0.11	N.S.
9003	Pathogenesis-related leaf protein 6	10.74 ± 1.53	N.S.	1.19 ± 0.68	N.S.
4408	AW040417.1 EST283281 tomato mixed elicitor	N.S.	N.S.	N.S.	0.51 ± 0.30
5001	Probable phospholipid hydroperoxide glutathione peroxidase (PR9-like)	27.61 ± 19.11	N.S.	–	–
5308	Triose phosphate isomerase (cytosolic isoform)	0.26 ± 0.05	–	–	–
5509	mRNA binding protein precursor	0.97 ± 0.48	N.S.	1.12 ± 0.02.	1.39 ± 0.51
4512	mRNA binding protein precursor	0.08 ± 0.01	N.S.	0.72 ± 0.15	0.54 ± 0.06
4301	Chaperonin 21 precursor	0.27 ± 0.02	7.70 ± 5.27	3.74 ± 0.01	7.86 ± 5.17
4803	Heat shock protein 70	0.13 ± 0.00	2.20 ± 1.36	1.41 ± 0.75	1.20 ± 0.08
7503	Isovaleryl-CoA dehydrogenase 1	0.85 ± 0.03	N.S.	0.87 ± 0.53	0.32 ± 0.04
6802	Subtilisin-like protease precursor	0.08 ± 0.00	–	–	1.27 ± 0.01
6804	Subtilisin-like protease precursor	0.64 ± 0.04	N.S.	0.90 ± 0.13	1.01 ± 0.26
4205	Temperature-induced lipocalin	12.63 ± 7.53	N.S.	0.07 ± 0.01	–
5201	EST470726 tomato shoot/meristem	0.28 ± 0.00	N.S.	8.63 ± 1.58	7.9 ± 5.22
6002	FS002771.1 Solanum melongena mRNA. clone	45.66 ± 28.4	N.S.	0.01 ± 0.00	0.26 ± 0.17
8101	BP903052.1 Solanum lycopersicum cDNA. clone	3.91 ± 1.45	N.S.	0.25 ± 0.08	0.42 ± 0.18

(−) Spots not evaluated due to lack of quantitative signal, no presence in all measured conditions, or too high quantitative variation between replicates.
(N.S.: non-significant differences).
*Ratios show the quantitative differences between the two expressed conditions and are calculated as means of three independent values for each spot from 2D gel electrophoresis analysis ± standard error.
  [a] Spot numbers refer to Fig. 6 identified either by fingerprint mass spectrometry MS (MALDI-TOF) or by MS/MS (MALDI TOF−TOF).

peroxidase activity [43].

The PR-9 family of peroxidases is likely to function in strengthening plant cell walls by catalyzing lignin deposition in reaction to microbial attack [64]. Our results showed that the first SA pre-treatment initiates a significant PR-9-like up-regulation, thus hinting at induced cell wall growth (to interfere with posterior viral spread inside the plant). Further study is needed to confirm that this effect is truly happening and may actually be the explanation for the delay of PVX-infection in SA-treated plants, as suggested by Ref. [19].

In general, pathogenesis related proteins increased just after SA pre-treatment only, concretely PR-6 and a PR-9-like proteins. No relevant variation was found (or was not evaluated due to lack of quantitative signal or no presence in all measured conditions) for either proteins in PVX-SPCP1 infected plants (Table 3) and after the initial SA effect (Table 2). PR-6 belongs to the sub-class of the serine proteinase inhibitor family, which may act by preventing completion of the viral replication cycles, thus conferring plant resistance as observed in our experiment [25,27].

Another protein, the subtilisin-like protease (subtilase) precursor significantly increased after two SA treatments (pre- and post-), whereas its levels were slightly decreased in PVX-infected plants. Proteases and protease inhibitors are important players of the so called plant-pathogen arms race. Previous studies have shown that in tomato the subtilases P69B and P69C were induced following pathogen attack and salicylic acid (SA) application [62]. In addition, subtilisin-like proteins have been identified during the tobacco-TMV mediated host resistance, suggesting important roles for plant virus defense responses (reviewed in Ref. [65]).

Superoxide dismutases (SODs) are enzymes known to participate in antioxidant networks [23]. SODs (CuZn-SOD and SOD-Mn) were found up-regulated in once SA treated plants (at 48 h post-treatment) [9]. Affirmed that changes in the expression levels of SOD proteins contribute to neutralization of the arsenal of ROS and organic hydroperoxides in plant tissues infected with virus. A similar variation was found in NAD(P)H-quinone oxidoreductase subunit H, which initially increased in abundance after the first SA treatment but later declined. These variations are among the

Table 3
Variation of altered protein levels between healthy controls (C) and Potato virus X (SPCP1 strain) − infected tomato (cv. Boludo) plants (V) treated or not with SA (dose 1.5 mM) in time. Sub-index numbers indicate sampling times; $T_2 = 7$ dpt/5 dpi and $T_4 = 14$ dpt/12 dpi. Only values where differences were consistent (variation coefficient $\leq 50\%$ among replicates, spots present in all measured conditions, expression ratios ≤ 0.5 or ≥ 2.0, and *in visu* validated spots) are shown (T_2 and T_4 correspond with two SA treatments, see Fig. 1).

SSP[a]	Protein	Ratio $(V/C)T_2$	Ratio $(V/C)T_4$	Ratio V_4/V_2	Ratio $(SA+V/V)T_2$	Ratio $(SA+V/V)T_4$	Ratio $(SA+V)T_4/(SA+V)T_2$
3103	ATP synthase epsilon chain	N.S.	N.S.	N.S.	N.S.	0.49 ± 0.15	N.S.
6206	Ethylene receptor 1	N.S.	6.76 ± 0.57	N.S.	N.S.	N.S.	N.S.
1603	chloroplast sedoheptulose-1.7-bisphosphatase	N.S.	N.S.	N.S.	N.S.	2.79 ± 0.71	–
1605	chloroplast sedoheptulose-1.7-bisphosphatase	N.S.	N.S.	2.72 ± 1.37	N.S.	N.S.	N.S.
7101	Peptidyl-prolyl cis-trans isomerase	N.S.	0.02 ± 0.001	–	–	N.S.	–
5207	Glutathione S-transferase. class-phi	N.S.	0.38 ± 0.12	N.S.	N.S.	N.S.	N.S.
3504	Ferredoxin–NADP reductase	–	11.66 ± 2.23	N.S.	N.S.	0.80 ± 0.10	0.79 ± 0.09
4404	Putative ferredoxin-NADP reductase	3.88 ± 0.54	4.21 ± 0.57	N.S.	N.S.	0.82 ± 0.07	0.27 ± 0.09
5403	Putative ferredoxin-NADP reductase (Fragment)	3.16 ± 0.53	3.02 ± 0.44	N.S.	–	0.84 ± 0.15	–
4507	NAD(P)H-quinone oxidoreductase subunit H	–	0.09 ± 0.03	–	–	0.16 ± 0.10	–
2203	Oxygen-evolving enhancer protein 2	N.S.	N.S.	0.22 ± 0.10	–	N.S.	–
9112	Photosystem II oxygen-evolving compl. prot. 3	N.S.	0.09 ± 0.03	N.S.	N.S.	N.S.	–
1609	Ribulose bisphosphate carbox./oxygenase activase	N.S.	N.S.	5.74 ± 3.49	0.72 ± 0.19	N.S.	N.S.
3612	Ribulose bisphosphate carbox./oxygenase activase	N.S.	N.S.	N.S.	N.S.	2.79 ± 0.64	0.18 ± 0.17
4502	Ribulose bisphosphate carbox./oxygenase activase	N.S.	N.S.	N.S.	–	0.92 ± 0.17	–
4603	Ribulose bisphosphate carbox./oxygenase activase	N.S.	N.S.	–	–	9.06 ± 6.41	–
4101	Ribulose bisphosphate carbox. small chain 3A/3C	–	–	N.S.	N.S.	1.35 ± 0.76	N.S.
4811	Ribulose bisphosphate carboxylase large chain	–	–	–	–	0.99 ± 0.59	N.S.
6809	Ribulose bisphosphate carboxylase large chain	N.S.	0.25 ± 0.03	–	–	N.S.	N.S.
7809	Ribulose bisphosphate carbox./oxygenase large subunit.	N.S.	7.50 ± 0.52	N.S.	N.S.	N.S.	–
5104	Wound-inducible carboxypeptidase precursor	N.S.	0.30 ± 0.08	N.S:	N.S.	N.S.	–
9003	Pathogenesis-related leaf protein 6	N.S.	0.01 ± 0.01	–	–	–	–
5509	mRNA binding protein precursor	0.46 ± 0.25	0.38 ± 0.07	N.S.	N.S.	N.S.	N.S.
4512	mRNA binding protein precursor	2.30 ± 0.82	2.01 ± 0.22	N.S.	N.S.	N.S.	N.S.
4301	Chaperonin 21 precursor	6.78 ± 3.97	4.43 ± 1.64	N.S.	N.S.	N.S.	N.S.
4803	Heat shock protein 70	0.91 ± 0.85	0.13 ± 0.03	–	–	N.S.	–
7503	Isovaleryl-CoA dehydrogenase 1	0.19 ± 0.01	0.09 ± 0.04	–	–	N.S.	–
6804	Subtilisin-like protease precursor	0.34 ± 0.21	0.68 ± 0.25	–	–	1.99 ± 0.23	N.S.
4205	Temperature-induced lipocalin	–	0.15 ± 0.12	–	–	N.S.	–
5201	EST470726 tomato shoot/meristem	18.26 ± 6.77	27.37 ± 2.64	N.S.	N.S.	N.S.	–
8101	BP903052.1 Solanum lycopersicum cDNA. clone	0.11 ± 0.05	0.19 ± 0.02	N.S.	N.S.	N.S.	–

(−) Spots not evaluated due to lack of quantitative signal, no presence in all measured conditions, or too high quantitative variation between replicates.
(N.S.: non-significant differences).
*Ratios show the quantitative differences between the two expressed conditions and are calculated as means of three independent values for each spot from 2D gel electrophoresis analysis ± standard error.
[a] Spot numbers refer to Fig. 6 identified either by fingerprint mass spectrometry MS (MALDI-TOF) or by MS/MS (MALDI TOF−TOF).

earliest temporal events following biotic and abiotic stress in plants [63]. NAD(P)H oxidase activity causes changes in the cellular pH, which can have an anti-pathogenic effect [57], so the increment after SA pre-treatment could have an important role controlling initial PVX. SPCP1-infection, considering that increased ROS in stomatal guard cells regulates gas exchange by promoting stomatal closure [33,34].

SA pre-treatment did not change ATPase levels but with time, the abundance of ATPases recovered and even increased. ATPases play a key role in the plant response to environmental stress. Research suggests that PM H + -ATPases are dynamically regulated during plant immune responses. Quantitative proteomic studies in a bacterial pathosystems suggest complex spatial and temporal modulation of PM H + -ATPase activity during early pathogen recognition events [17], consistent with our results. A tendency is confirmed for PM H + -ATP under PVX-SPCP1 infection (see Supplementary Table S1), but not significantly.

Our findings are consistent with other studies that affirm that SA pre-treatment confers thermotolerance [13,14], as the level of temperature-induced lipocalin (TIL1), an essential component for thermotolerance [10] was significantly altered after the first SA treatment, previous to virus inoculation. The heat shock protein 70 (HSP70), a chaperonin also involved in thermotolerance [37,60], was first down-regulated, but significantly increased in subsequent SA post-inoculations treatments. In the case of PVX-SPCP1-infected plants, nothing happened in the case of TIL1; however, a chaperonin 21 precursor was strongly up-regulated by PVX-SPCP1 infection and HSP70 increased because of SA treatments (see Tables 2 and 3). Chaperonin proteins are considered necessary or essential in some viral infections, so they participate in the construction of a viral replication complex and play various roles during viral infection [4,28]. The association between heat shock proteins up-regulation, thermotolerance and viral infection has been referenced in different viral pathosystems [32].

To conclude, we can say that proteomic analysis helps to understand the dynamic pattern of protein expression during different processes at different times, especially in overlapping effects, as PVX-SPCP1 infected plants indeed have reduced photosynthesis and SA offsets the impact of virus infection after two treatments (pre- and post-inoculation). PVX-SPCP1 induced symptoms in tomato plants disappeared after all SA treatments. The tomato defense response is enhanced following SA pre-treatment. Both SA-treatment alone and SA-treatment coupled with PVX-SPCP1 infection induce plant stress responses, as evidenced by alterations in abundance of particular proteins. Further detailed and functional analysis of proteins exhibiting expression changes would elucidate their individual roles during the infection.

Statement of author contributions

This work is multidisciplinary and therefore, the authors have contributed differently for different sections. Everyone has

participated and given their opinion when correcting the manuscript and in discussion of the results.

Listed below are the detailed areas in which the other authors have intervened.

Ana Isabel Cueto-Ginzo and **Vicente Medina** were responsible for the experimental design, drafting the manuscript, interpretation of results and monitoring of all the essays in this work. Ana Isabel also actively participated in all the technical work. **Richard M. Bostock** was involved in the interpretation of results and the final revision of the English and general content. **Juan Pedro Ferrio** and **Luis Serrano** are experts in plant physiology, thus contributing to the statistical analysis and the interpretation of physiological data. **Ricardo Rodriguez** was involved in the plant root analysis and interpretation of obtained data. **Laura Arcal** and **Walter P. Luzuriaga** supported all the work throughout the experimental stage by performing protein extractions, sample collection, and preparation of buffers for proteomic studies. **Tania Falcioni** and **Maria Angeles Achón** gave relevant advice during the development of experimental design, assisted in the supervision of all trials and actively participated in sample collection when necessary; most specifically with virus inoculation and ELISA procedures.

Appendix A. Supplementary data

Supplementary data related to this article can be found at http://dx.doi.org/10.1016/j.pmpp.2015.11.003.

References

[1] M.J. Adams, J.F. Antoniw, M. Bar-Joseph, A.A. Brunt, T. Candresse, G.D. Foster, G.P. Martelli, R.G. Milne, C.M. Fauquet, The new plant virus family *Flexiviridae* and assessment of molecular criteria for species demarcation, Archives Virol. 149 (2004) 1045—1060.

[2] T. Aminalah, Z. Maryam, T. Asma, D. Akbar, K.H. Mina, Role of salicylic acid in resistance to plant viruses, Genet. 3rd Millenn. 8 (2011) 2203—2212.

[3] E.A. Ananieva, K.N. Christov, L.P. Popova, Exogenous treatment with salicylic acid leads to increased antioxidant capacity in leaves of barley plants exposed to paraquat, J. Plant Physiol. 161 (2004) 319—328.

[4] F. Aparicio, C.L. Thomas, C. Lederer, Y. Niu, D. Wang, A.J. Maule, Virus induction of heat shock protein 70 reflects a general response to protein accumulation in the plant cytosol, Plant Physiol. 138 (2005) 529—536.

[5] M. Arfan, H.R. Athar, M. Ashraf, Does exogenous application of salicylic acid through the rooting medium modulate growth and photosynthetic capacity in two differently adapted spring wheat cultivars under salt stress? J. Plant Physiol. 6 (4) (2007) 685—694.

[7] R.R. Barkosky, F.A. Einhellig, Effects of salicylic acid on plant water relationship, J. Chem. Ecol. 19 (1993) 237—247.

[8] Y. Bektas, T. Eulgem, Synthetic plant defense elicitors, Front. Plant Sci. 5 (804) (2015) 1—17.

[9] J. Casado-Vela, S. Sellés, R.B. Martínez, Proteomic analysis of tobacco mosaic virus-infected tomato (*Lycopersicon esculentum* M.) fruits and detection of viral coat protein, Proteomics (Suppl. 1) (2006) S196—S206.

[10] W.T. Chi, R.W.M. Fung, H.C. Liu, C.C. Hsu, Y.Y. Charng, Temperature-induced lipocalin is required for basal and acquired thermotolerance in *Arabidopsis*, Plant Cell Environ. 32 (2009) 917—927.

[11] S. Cho, W. Cho, H. Choi, K. Kim, Cis-acting element (SL1) of *Potato virus X*

[12] M.F. Clark, A.N. Adams, Characteristics of the microplate method of enzyme linked immune-sorbent assay for the detection of plant viruses, J. General Virol. 34 (1977) 475—483.

[13] S.M. Clarke, S.M. Cristescu, O. Miersch, F.J.M. Harren, C. Wasternack, L.A.J. Mur, Jasmonates interact with salicylic acid to confer basal thermotolerance in *Arabidopsis thaliana*, New Phytol. 182 (1) (2009) 175—187.

[14] S.M. Clarke, L.A. Mur, J.E. Wood, I.M. Scott, Salicylic acid dependent signaling promotes basal thermotolerance but is not essential for acquired thermotolerance in *Arabidopsis thaliana*, Plant J. 38 (3) (2004) 432—447.

[15] W. Cleveland, Robust locally weighted regression and smoothing scatterplots, J. Am. Stat. Assoc. 74 (368) (1979) 829—836.

[16] A.I. Cueto-Ginzo, F. Aparisi, M.A. Achón, V. Pallás, L. Arcal, S. Lade, V. Medina, Characterization of a new Spanish *Potato virus X* strain inducing symptoms in tomato, J. Plant Pathol. 97 (2) (2015) 369—372.

[17] J.M. Elmore, G. Coaker, The role of the plasma membrane H+-ATPase in plant-microbe interactions, Mol. Plant 4 (3) (2011) 416—427.

[18] M.A. El-Tayeb, Response of barley grains to the interactive effect of salinity and salicylic acid, Plant Growth Regul. 45 (2005) 215—224.

[19] T. Falcioni, J.P. Ferrio, A.I. Cueto, J. Giné, M.A. Achón, V. Medina, Effect of salicylic acid treatment on tomato plant physiology and resistance to *Potato virus X* infection, Eur. J. Plant Pathol. 138 (2014) 331—345.

[20] J.P. Ferrio, A. Pou, I. Florez-Sarasa, A. Gessler, N. Kodama, J. Flexas, M. Ribas-Carbó, The Péclet effect on leaf water enrichment correlates with leaf hydraulic conductance and mesophyll conductance for CO_2, Plant Cell Environ. 35 (3) (2012) 611—625.

[21] J. Flexas, M. Barbour, O. Brendel, H. Cabrera, M. Carriqui, A. Diaz-Espejo, Mesophyll diffusion conductance to CO_2: an unappreciated central player in photosynthesis, Plant Sci. 193—194 (2012) 70—84.

[22] L. Gallego-Giraldo, L. Escamillo-Trevino, L.A. Jackson, R.A. Dixon, SA mediates the reduced growth of lignin down-regulated plants, PNAS 108 (51) (2011) 20814—20819.

[23] S.S. Gill, N. Tuteja, Reactive oxygen species and antioxidant machinery in abiotic stress tolerance in crop plants, Plant Physiol. Biochem. 48 (2010) 909—930.

[24] A. Gunes, A. Inal, M. Alpaslan, F. Eraslan, E.G. Bagci, N. Cicek, Salicylic acid induced changes on some physiological parameters symptomatic for oxidative stress and mineral nutrition in maize (*Zea mays* L.) grown under salinity, J. Plant Physiol. 164 (2007) 728—736.

[25] R. Gutiérrez-Campos, J. Torres-Acosta, L. Saucedo-Arias, M. Gómez-Lim, The use of cysteine proteinase inhibitors to engineer resistance against potyviruses in transgenic tobacco plants, Nat. Biotechnol. 17 (1999) 1223—1226.

[26] V. Haake, R. Zrenner, U. Sonnewald, M. Stitt, A moderate decrease of plastid aldolase activity inhibits photosynthesis, alters the levels of sugars and starch, and inhibits growth of potato plants, Plant J. 14 (2) (1998) 147—157.

[27] H. Habib, M. Fazili, Plant proteasse inhibitors: a defense strategy in plants, Biotechnol. Mol. Biol. Rev. 2 (3) (2007) 68—85.

[28] A. Hafren, D. Hofius, G. Ronnholm, U. Sonnewald, K. Makinen, HSP70 and its cochaperone CPIP promote potyvirus infection in *Nicotiana benthamiana* by regulating viral coat protein functions, Plant Cell 22 (2010) 523—535.

[29] S. Hayat, B. Ali, A. Ahmad, Salicylic acid: biosynthesis, metabolism and physiological role in plants, in: S. Hayat, A. Ahmad (Eds.), Salicylic Acid: a Plant Hormone, Springer, Dordrecht, The Netherlands, 2007, pp. 1—14.

[30] M. Heil, R.M. Bostock, Induced systemic resistance (ISR) against pathogens in the context of induced plant defenses, Ann. Bot. 89 (5) (2002) 503—512.

[31] K. Janda, E. Hideg, G. Szalai, L. Kovács, T. Janda, Salicylic acid may indirectly influence the photosynthetic electron transport, J. Plant Physiol. 169 (2012) 971—978.

[32] S. Jiang, Y. Lu, K. Li, L. Lin, H. Zheng, F. Yan, J. Chen, Heat shock protein 70 is necessary for rice stripe virus infection in plants, Mol. Plant Pathol. 15 (9) (2014) 907—917.

[33] J.H. Joo, S. Wang, J.G. Chen, A.M. Jones, N.V. Fedoroff, Different signaling and cell death roles of heterotrimetric G protein α and β subunits in the *Arabidopsis* oxidative stress response to ozone, Plant Cell 17 (2005) 957—970.

[34] J.M. Kwak, I.C. Mori, Z.M. Pei, N. Leonhardt, M.A. Torres, J.L. Dangl, R.E. Bloom, S. Bodde, J.D. Jones, J.I. Schroeder, NADPH oxidase *AtrbohD* and AtrbohF genes function in ROS-dependent ABA signaling in *Arabidopsis*, EMBO J. 22 (2003) 2623—2633.

[35] A. Larqué-Saavedra, Stomatal closure in response to acetylsalicylic acid treatment, Z. für Pflanzenphysiol. 93 (1979) 371—375.

[36] R. Larson, W. Wintermantel, A. Hill, L. Fortis, A. Nunez, Proteome changes in sugar beet in response to Beet necrotic yellow vein virus, Physiological Mol. Plant Pathol. 72 (2008) 62—72.

[37] J.H. Lee, F. Schöffl, An Hsp70 antisense gene affects the expression of HSP70/HSC70, the regulation of HSF, and the acquisition of thermotolerance in transgenic *Arabidopsis thaliana*, Mol. General Genet. 252 (1996) 11—19.

[38] W.-S. Lee, Fu Sh-F, J. Verchot-Lubicz, J.P. Carr, Genetic modification of alternative respiration in *Nicotiana benthamiana* affects basal and salicylic acid-induced resistance to *Potato virus X*, BMC Plant Biol. 11 (2011) 41.

[39] K. Lehto, M. Tikkanen, J.-B. Hinart, V. Paakkarinen, E.-M. Aro, Depletion of the photosystem II core complex in mature tobacco leaves infected by the Falvum strain of *Tobacco mosaic virus*, Mol. Plant Microbe Interact. 16 (2003) 1135—1144.

[40] A.M. Lennon, U.H. Neuenschwander, M. Ribas-Carbo, L. Giles, J.A. Ryals,

J.N. Siedow, The effects of salicylic acid and tobacco mosaic virus infection on the alternative oxidase of tobacco, Plant Physiol. 11 (5) (1997) 783—791.

[41] G. Lohaus, H.W. Heldt, C.B. Osmond, Infection with phloem limited *Abutilon mosaic virus* causes localized carbohydrate accumulation in leaves of *Abutilon striatum*: relationships to symptom development and effects on chlorophyll fluorescence quenching during photosynthetic induction, Plant Biol. 2 (2000) 161—167.

[42] Y. Lu, D. Liao, J. Pu, Y. Qi, Y. Xie, Proteome analysis of resistant and susceptible Cavendish banana roots following inoculation with *Fusarium oxysporum* f.sp. cubense, Physiological Mol. Plant Pathol. 84 (2013) 163—171.

[43] C. Martinez, F. Blanc, E. Le Claire, O. Besnard, M. Nicole, J.-C. Baccou, Plant Physiol. 127 (1) (2001) 334—344.

[44] Y. Miyagawa, M. Tamoi, S. Shigeoka, Overexpression of a cyanobacterial fructose-1,6-/sedoheptulose-1, 7-bisphosphatase in tobacco enhances photosynthesis and growth, Nat. Biotechnol. 19 (2001) 965—969.

[45] K. Miura, Y. Tada, Regulation of water, salinity and cold stress responses by salicylic acid, Front. Plant Sci. 5 (4) (2014) 1—12.

[46] A.M. Murphy, J.P. Carr, Salicylic acid has cell-specific effects on *Tobacco mosaic virus* replication and cell-to-cell movement, Plant Physiol. 128 (2002) 552—563.

[47] E. Nyalugwe, C. Wilson, B. Coutts, R. Jones, Biological properties of *Potato virus X* in potato: effects of mixed infection with *Potato virus S* and resistance phenotypes in cultivars from three continents, Plant Dis. 96 (2012) 43—54.

[48] H. Olçer, J.C. Lloyd, C.A. Raines, Photosynthetic capacity is differentially affected by reductions in sedoheptulose-1,7-bisphosphatase activity during leaf development in transgenic tobacco plants, Plant Physiol. 125 (2) (2001) 982—989.

[49] R.C. O'Malley, F.I. Rodriguez, J.J. Esch, B.M. Binder, P. O'Donnell, H.J. Klee, A.B. Bleecker, Ethylene-binding activity, gene expression levels, and receptor system output for ethylene receptor family members from *Arabidopsis* and tomato, Plant J. 41 (2005) 651—659.

[50] M.L. Pérez-Bueno, J. Rahoutei, C. Sajnani, I. García-Luque, M. Barón, Proteomic analysis of the oxygen — evolving complex of photosystem II under biotic-stress. Studies on *Nicotiana benthamiana* infected with tobamoviruses, Proteomics 4 (2004) 415—418.

[51] X. Qu, G.E. Schaller, Requirement of the histidine kinase domain for signal transduction by the ethylene receptor ETR1, Plant Physiol. 136 (2004) 2961—2970.

[52] V.K. Rai, S.S. Sharma, S. Sharma, Reversal of ABA—induced Stomatal closure by phenolic compounds, J. Exp. Bot. 37 (1986) 129—134.

[53] M. Rivas-San Vicente, J. Plasencia, Salicylic acid beyond defence: its role in plant growth and development, J. Exp. Bot. 62 (10) (2011) 3321—3338.

[54] M. Rockenbach, J. Boneti, G. Cangahuala-Inocente, M. Andrade Gavioli-Nascimento, M. Guerra, Histological and proteomics analysis of apple defense responses to the development of *Colletotrichum gloeosporioides* on leaves, Physiological Mol. Plant Pathol. 89 (2015) 97—107.

[55] D.M. Rosenthal, A.M. Locke, M. Khozaei, C.A. Raines, S.P. Long, D.R. Ort, Over-expressing the C3 photosynthesis cycle enzyme sedoheptulose-1-7 bisphosphatase improves photosynthetic carbon gain and yield under fully open air CO2 fumigation (FACE), BMC Plant Biol. 11 (2011) 123.

[56] B. Sampol, J. Bota, D. Riera, H. Medrano, J. Flexas, Analysis of the virus-induced inhibition of photosynthesis in malmsey grapevines, New Phytol. 160 (2003) 403—412.

[57] A.W. Segal, The function of the NADPH oxidase of phagocytes and its relationship to other NOXs in plants, invertebrates and mammals, Int. J. Biochem. Cell Biol. 40 (2008) 604—618.

[58] D.P. Singh, C.A. Moore, A. Gilliland, J.P. Carr, Activation of multiple antiviral defense mechanisms by salicylic acid, Mol. Plant Pathol. 5 (2004) 57—63.

[59] T. Stare, Ž. Ramšak, A. Blejec, K. Stare, N. Turnšek, W. Weckwerth, S. Wienkoop, D. Vodnik, K. Gruden, Bimodal dynamics of primary metabolism-related responses in tolerant potato-*Potato virus* Y interaction, BMC Genomics 16 (1) (2015) 716, http://dx.doi.org/10.1186/s12864-015-1925-2.

[60] P.H. Su, H.M. Li, *Arabidopsis* stromal 70-kD heat shock proteins are essential for plant development and important for thermotolerance of germinating seeds, Plant Physiol. 146 (2008) 1231—1241.

[61] M. Tian, Z. Sasvani, P.A. Gonzalez, G. Friso, E. Rowland, X.M. Liu, K.J. van Wijk, P.D. Nagy, D. Klessig, Salicylic acid inhibits the replication of *Tomato Bushy Stunt Virus* by directly targeting a host component in the replication complex, Mol. Plant Microbe Interact. 28 (4) (2015) 379—386.

[62] P. Tornero, V. Conejero, P. Vera, Primary structure and expression of a pathogen-induced protease (PR-P69) in tomato plants: similarity of functional domains to subtilisin-like endoproteases, Proc. Natl. Acad. Sci. U. S. A. (PNAS) 93 (1996) 6332—6337.

[63] M.A. Torres, J.L. Dangl, Functions of the respiratory burst oxidase in biotic interactions, abiotic stress and development, Curr. Opin. Plant Biol. 8 (4) (2005) 397—403.

[64] L.C. Van Loon, E.A. Van Strien, The families of pathogenesis-related proteins, their activities, and comparative analysis of PR-1 type proteins, Physiological Mol. Plant Pathol. 55 (1999) 85—97.

[65] A. Vartapetian, A. Tuzhikov, N. Chichkova, M. Taliansky, T. Wolpert, A plant alternative to animal caspases: subtilisin-like proteases, Cell Death Differ. 18 (2011) 1289—1297.

[67] K. Webb, W. Wintermantel, N. Kaur, J. Prenni, C. Broccardo, L. Wolfe, L. Hladky, Differential abundance of proteins in response to Beet necrotic yellow vein virus during compatible and incompatible interactions in sugar beet containing Rz1 or Rz2, Physiological Mol. Plant Pathol. 91 (2015) 96—105.

[68] L.J. Wu, Z.P. Han, S.X. Wang, X.T. Wang, A.G. Sun, X.F. Zu, Y.H. Chen, Comparative proteomic analysis of the plant—virus interaction in resistant and susceptible genotypes of maize infected with sugarcane mosaic virus, J. Proteomics 89 (2013) 124—140.

[69] S. Berger, A.K. Sinha, T. Roitsch, Plant physiology meets phytopathology: plant primary metabolism and plant—pathogen interactions, J. Exp. Bot. 58 (15-16) (2007) 4019—4026.